Please cite the Published Version

PAPER • OPEN ACCESS

Metal Complexes of Multidentate N_2S_2 Heterocyclic Schiff-base Ligands;Formation, Structural Characterisation and Biological Activity

To cite this article: Baidaa K Al-Rubaye *et al* 2021 *J. Phys.: Conf. Ser.* **1879** 022074

View the article online for updates and enhancements.

Metal Complexes of Multidentate N_2S_2 Heterocyclic Schiff-base Ligands;Formation, Structural Characterisation and Biological Activity

Baidaa K Al-Rubaye [1], Mohamad J. Al-Jeboori [1*] and Herman Potgieter [2]

[1] Department of Chemistry, College of Education for Pure Science (Ibn Al-Haitham), University of Baghdad, Baghdad, Iraq.
[2] Division of Chemistry and Environmental Science, Manchester Metropolitan University, Manchester, M1 5GD, UK.

*E-mail: mohamadaljeboori@yahoo.com

Abstract: The synthesis of ligands with N_2S_2 donor sets that include imine, an amide, thioether, thiolate moieties and their metal complexes were achieved. The new Schiff-base ligands; N-(2-((2,4-diphenyl-3-azabicyclo[3.3.1]nonan-9-ylidene)amino)ethyl)-2-((2-mercaptoethyl)thio)- acetamide (H_2L^1) and N-(2-((2,4-di-p-tolyl-3-azabicyclo[3.3.1]nonan-9-ylidene)amino)ethyl)-2-((2-mercaptoethyl)thio) acetamide (H_2L^2) were obtained from the reaction of amine precursors with 1,4-dithian-2-one in the presence of triethylamine as a base in the $CHCl_3$ medium. Complexes of the general formula $K_2[M(Ln)Cl_2]$, (where: M = Mn (II), Co(II) and Ni(II)) and [M(Ln)], (where: M = Cu(II), Zn(II) and Cd(II); n =1-2, expect $[Cu(HL^2)Cl]$) were isolated. The entity of ligands and complexes including their purity were confirmed using elemental microanalysis (C.H.N.S), atomic absorption (A.A), chloride content, conductivity measurement's, melting point and thermal analysis technique. The molecular structures were elucidated with FT-IR, UV-Vis, magnetic susceptibility, ^{1}H- and ^{13}C-NMR and mass spectroscopy. The synthesised compounds were evaluated for their activity against bacterial strains (G+ and G-) and fungi species. The tested compounds indicated that; the ligands have not shown any antimicrobial activity against *Escherichia coli*. The Cd(II) complexes, for ligands H_2L^1 and H_2L^2, display the higher antimicrobial activity, compared with the other complexes. The H_2L^1 and H_2L^2 have not shown any activity against *Candida albicans*. All complexes for ligands (H_2L^1 and H_2L^2) exhibited less activity against *Candida albicans*, compared with other types of fungi.

Keywords: Schiff-bases, N_2S_2 ligand system, Metal complexes, Structural characterisation, Biological activity.

1. Introduction

Compounds incorporate nitrogen and sulfur in their frameworks are a class of organic species that attracted a range of chemist researchers (organic, inorganic and bioinorganic chemists) [1]. The impact of these species on chemistry stimulated researches to investigate and implementing a range of synthetic protocols to increase yields and stability of these materials. These species have shown a range of potential applications, including their role as useful chelating agents for radio-metals of transition and representative elements [2]. They have also used as biomedical agents, in radiopharmaceutical [2], medicine [3] and as a mimic for bioactive molecules, in catalysis, analytical chemistry, coordination chemistry [4], environmental, materials and supramolecular chemistry [5]. Mannich-bases are an important organic species that pronounced a range of uses and applications in chemistry. Compounds derived from 2,4-bis(R-phenyl)-3-azabicyclo[3.3.1]nonan-9-one are interesting materials that used as organic reagents in the fabrication of natural-based blocks including the synthesis of

phenanthridine-based compounds [6,7]. Further, compounds include N_2S_2 systems are remarkable materials that played a part in the expansion of chemistry and nuclear medicine [8]. Thus, the formation of functionalised Mannich-bases with N, S atoms should be an important class of compounds. They provide a flexible *hard/soft* system, upon acting as a chelating ligand to the metal centre. In this work, we describe the synthesis and characterisation of two multidentate N_2S_2 heterocyclic ligands N-(2-((2,4-diphenyl-3-azabi cyclo[3.3.1] nonan-9-ylidene)amino)ethyl)-2-((2-mercapto ethyl)thio)acetamide (H_2L^1) and N-(2-((2,4-di-p-tolyl-3-azabicyclo[3.3.1]nonan-9-ylidene)amino)ethyl)-2-((2-mercapto ethyl)thio)acetamide (H_2L^2) and their metal complexes. The anti-bacterial and anti-fungi behaviour of ligands and their complexes were also investigated.

2. Experimental

2.1. Materials and methods

All reagents in this work were commercially available and used without further purification. 1,4-Dithian-2-one and ligands were obtained by a reported method [8,9].

2.2. Physical measurements

A Heraeus instrument (Vario EL) and a Perkin-Elmer 2400 Series-II analyser were used to obtain elemental analyses (C.H.N.S) at Materials Research Centre, Ministry for Science and Technology, Baghdad, IRAQ. Uncorrected melting points were recorded using an electro-thermal Stuart SMP40 apparatus. FT-IR spectra were measured as KBr discs using a Biotic 600 FT-IR spectrophotometer in the range 4000-400 cm^{-1} FTIR and as CsI discs in the range 4000-200 cm^{-1} on a Shimadzu 8400s FT-IR at College of Science, University of Baghdad. Electronic spectra were measured from 200-1100 nm for 10^{-3} M solutions in DMSO at room temperature with (UV-Vis) spectrophotometer type Shimadzu 1800, using quartz cell of 1.0 cm length. The measurements were obtained at Ibn Sina Company, Ministry of Industry, Baghdad, Iraq. Mass spectra were obtained as Electrospray (ES) using an LTQ-FT mass spectrometer (Thermo Fisher Scientific). The spectra were recorded at the University of Manchester Metropolitan, UK. The spectral data were recorded in the positive mode. NMR spectra (^1H, ^{13}C-NMR) were recorded in DMSO-d_6 solutions using a Brucker-400 MHz and a JEOL-400 MHz for ^1HNMR and 100.61 MHz for ^{13}C-NMR, respectively, and TMS was used as an internal standard for ^1HNMR measurement. The samples were recorded at the University of Manchester Metropolitan, UK and Isfahan University, Islamic Republic of Iran. Metals were determined using a Shimadzu atomic absorption spectrophotometer (F.A.A) 680G. Chloride was determined using a 686-titro processor-665 Dosimat-Metrohm Swiss. in Ibn Sina Company, Ministry of Industry Baghdad, Iraq. Conductivity measurements were made with DMSO solutions using a Eutech Instruments Co, 150 digital conductivity meter, and magnetic moments were determined at 298 k with a Sherwood Scientific magnetic susceptibility balance. Thermal analyses were performed under an argon atmosphere on an STA PT-1000 Linseis company /Germany with a heating rate of 10 ºC/min. at College of Education for Pure Science (Ibn Al-Haitham), University of Baghdad. The evaluation of ligands and their metal complexes against four bacterial strains *(Escherichia coli, Pseudomonas aeruginosa, Staphylococcus aureus and Bacillus stubtilis)* and four fungi species (*Candida albicans, Candida glabrata, Candida tropicalis and Candida parapsilsis*) were performed using agar-well diffusion. The results were recorded at College of Science, Baghdad University and at College of Education for Pure Science (Ibn Al-Haitham), University of Baghdad.

2.3. Synthesis
2.3.1. Preparation of precursors (M₁, M₂, A₁ and A₂)

The preparation of M_1 and M_2 was performed according to a published method [10,11] and the preparation of A_1 and A_2 was achieved using a reported method [12].

2.3.1.1. Preparation of (1R,2R,4R,5S)-2,4-diphenyl-3-azabicyclo[3.3.1]nonan-9-one (M₁)

A solution of benzaldehyde (1.33ml, 13mmol), ammonium acetate (0.5g, 6.500mmol) and cyclohexanone (0.674ml, 6.500mmol) [2:1:1] in ethanol (20ml) was mixed together. The reaction mixture was allowed heating between 30-40 ºC for 6h, during which time a yellow solid was formed. However, upon using MeOH medium for 4h reflux the reaction yielded an identical compound. The solid was collected by filtration, washed with ethanol (5ml), and diethylether (10ml) and then dried under vacuum. Yield: 1.26g (93%), m.p = 108-110 ºC. FT-IR data (cm^{-1}), 3313 ν(N–H), 3032 ν(C–H)$_{arom}$, 2920 and 2850 ν(C–H)$_{alip}$, 1716 ν(C=O), 1581 and 1558 ν(C=C), 1492 ν(N–H). NMR data (ppm), ^{1}H (400 MHz, DMSO-d$_6$): δ_H = 1.60 (2H, m, C$_{10}$-H); 1.76 (4H, quar, 3.6 Hz, J_{HH} = 9.6 Hz, C$_{9,9}$`-$H$); 2.60 (2H, dd, $J_{HH}$ = 6 Hz, C$_{8,8}$`-H); 2.80 (2H, t, J_{HH} = 4.8 Hz, C$_{7,7}$`-$H$); 7.80 ppm (1H, s, $N$-$H$); 7.02 and 7.11 (C$_{1,1}$`-H; 2H, t, J_{HH} = 5.2 Hz) and (C$_{2,2}$`, $_{6,6}$`-H; 4H, t, J_{HH} = 5.2 Hz), respectively; 7.43 ppm (4H, d, J_{HH} = 6 Hz) was assigned to (C3,3`, 5,5`-H); ^{13}C NMR (100.63 MHz, DMSO-d$_6$): δ_c = 22.89 (C$_{10}$), 25.61 (C$_{9,9}$`), 55.69 (C$_{7,7}$`), 58.93 (C$_{8,8}$`), 124.09 (C$_{1,1}$`), 131.08 (C$_{2,2}$`, $_{6,6}$`) and (C$_{3,3}$`, $_{5,5}$`), 139.37 (C$_{4,4}$`), 203.40 (C=O). The electrospray (+) mass spectrum of M$_1$ shows no molecular ion peak for M$_1$. Peak detected at m/z = 266.2844 amu assigned to [M-(C$_2$H$_2$)+H)]$^+$ for C$_{18}$H$_{20}$NO, requires = 266.1539. The other peaks detected at m/z = 240.2844, 174.1106 and 107.0409 were assigned to [(M-C$_2$H2+C$_2$)]$^+$, [(M-C$_2$H+C$_2$+C$_6$H)]$^+$ and [(M-C$_2$H+C$_2$+C$_6$H+C$_4$H$_{14}$)]$^+$.

2.3.1.2. Preparation of (1R,2R,4R,5S)-2,4-di-p-tolyl-3-azabicyclo[3.3.1]nonan-9-one (M$_2$)

The method used to prepare M$_2$ was analogous to the starting material M$_1$, but with the used of 4-methylbenzaldehyde instead of benzaldehyde. The amounts of other reagents used were adjusted accordingly, and a similar workup procedure was used to give compound M$_2$ as a pale-yellow solid. Yield: 1.53g (54 %) , m.p. = 168-170 ºC. FT-IR data (cm^{-1}), 3298 ν(N–H), 3020 ν(C–H)$_{arom}$, 2858 and 2927 ν(C–H)$_{alip}$, 1705 ν(C=O), 1577 and 1550 ν(C=C), 1512 ν(N–H). NMR data (ppm), ^{1}H (400 MHz, DMSO-d$_6$): δ_H = 1.57 (2H, m, C$_{10}$-H); 1.67 (4H, m, C$_{9,9}$`-$H$); 1.77 and 1.79 (2H, d, $J_{HH}$ = 6 Hz, C$_{8,8}$`-H); 2. 71 (2H, t, J_{HH} = 5.6 Hz, C$_{7,7}$`-$H$); 2.91 ppm (6H, s, *2CH$_3$*); 4.36 (1H, s, $N$-$H$); 7.38 (4H, d, $J_{HH}$ = 7.2 Hz, (C$_{2,2}$`, $_{6,6}$`-$H$); and 7.43 ppm (4H, d, $J_{HH}$ = 7.2 Hz (C$_{3,3}$`, $_{5,5}$`-$H$). $^{13}$C NMR (100.63 MHz, DMSO-d$_6$): $\delta_c$ = 23.75 (C$_{10}$); 25.98 (C$_{9,9}$`); 44.61 (C methyl); 56.19 (C$_{8,8}$`); 58.79 (C$_{7,7}$`); 124.93 (C$_{3,3}$`, $_{5,5}$`); 126.71 (C$_{2,2}$`, $_{6,6}$`); 135.61(C$_{1,1}$`); 138.93 (C$_{4,4}$`) and 209.69 (C=O). The electrospray (+) mass spectrum of M$_2$ shows the molecular ion peak for M$_2$ at m/z = 319.0421 amu for C$_{22}$H$_{25}$NO, requires = 319.1936. Peaks recorded at m/z = 275.1434 and 151.4732 amu attributed to [M-(CH$_3$CH$_2$CH$_3$)]$^+$ and [M-(CH$_3$CH$_2$CH$_3$)+(C$_{10}$H$_4$)]$^+$.

2.3.1.3. Preparation of 2-(((1R,2S,4R,5S,E)-2,4-diphenyl-3-azabicyclo[3.3.1]nonan-9-ylidene)amino)ethan-1-amine (A$_1$)

A solution of ethylenediamine (0.160g, 2.663mmol) dissolved in ethanol (20ml) was added to a mixture of M$_1$ (0.8g, 2.747mmol) in ethanol (20ml). The reaction mixture was treated with 2ml of concentration hydrochloride acid, and then allowed to reflux for 6h. The reaction mixture was left for a slow evaporation and yellow crystals were obtained that isolated by filtration, washed with cold ethanol (5ml) and diethylether (10ml) and then dried under vacuum. Yield: 0.104g (65%), m.p = 194-196 ºC. FT-IR data (cm^{-1}), 3309 and 3248 ν(N–H), 1639 ν(C=N), 1504 δ(N–H), 119 ν(C–N). NMR data (ppm), ^{1}H NMR (400 MHz, DMSO-d$_6$): δ_H = 1.24 (6H, m, C$_{9,9}$` and C$_{10}$-$H$); 1.75 (2H, m, C$_{12}$-$H$); 2.28-2.41 (5H, m, C$_{8,8}$`,C$_{11}$-H and N-H); 3.16 (2H, d, J_{HH} = 7.6 Hz, C$_{7,7}$`-$H$); 7.25 (C$_{1,1}$`-H; 2H, t, J_{HH} = 4.4 Hz); 7.35 (C$_{2,2}$`, $_{6,6}$`-H; 4H, t, J_{HH} = 4.4 Hz); 7.46 (4H, dd, J_{HH} = 3.6 and 7.3 Hz) (C$_{3,3}$`, $_{5,5}$`-H). ^{13}C NMR (100.63 MHz, DMSO-d$_6$): δ_c = 23.80 (C$_{9, 9}$`); 27.83 (C$_{10}$); 28.80 (C$_{8, 8}$`); 35.39(C$_{7,7}$`); 46.82 (C$_{12}$); 49.44(C$_{11}$); 122.35 (C$_{1,1}$`); 127.08 (C$_{3,3}$`, C$_{2,2}$`); 127.24 (C$_{6,6}$`); 142.49 (C$_{4,4}$`);152.49 (C=N). The electrospray (+) mass spectrum of A$_1$ revealed a peak at m/z = 333.1042 amu assigned to (M)$^+$ for C$_{22}$H$_{27}$N$_3$, requires = 333.2205 and the following fragments at 304.1548 and 264.1742 amu were related to [M-CH$_3$N]$^+$ and [M-(CH$_3$N+C$_3$H$_4$)]$^+$, respectively.

2.3.1.4 Preparation of 2-(((1R,2S,4R,5S,E)-2,4-di-p-tolyl-3-azabicyclo[3.3.1]nonan-9-ylidene)amino)ethan-1-amine (A$_2$)

An analogues method for the isolation of precursor A_1 was used to prepare A_2, but M_2 was used in place of M_1 and other reagents were adjusted accordingly. A yellow solid was obtained, yield = 0.2155g (75 %), m.p. = 113-115 ºC. FT-IR data (cm^{-1}), 3421 ν(N–H), 1658 ν(C=N), 1508 δ(N–H), 1311 ν(C–N). NMR data (ppm), ^{1}H NMR (400 MHz, DMSO-d$_6$): δ_H = 1.18 (6H, m, C$_{9,9`}$, C$_{10}$ -H); 1.55 (2H, m, C$_{12}$-H); 2.20-2.25 (5H, m, C$_{8,8`}$, C$_{11}$-H) and N-H; 3.10 (2H, d, J_{HH} = 5.2 Hz C$_{7,7`}$-H); 3.76 (6H, s, 2 x CH$_3$); = 7.02 (4H, d, $J_{HH}$ = 7.6 Hz, C$_{2,2`}$, $_{6,6`}$-H); 7.70 (4H, d, $J_{HH}$ = 7.6 Hz, C$_{3,3`, 5,5`}$-H). $^{13}$C NMR (100.63 MHz, DMSO-d$_6$): $\delta_c$ = 21.82 (C$_{methyl}$); 22.02 (C$_{9, 9`}$); 24.50 (C$_{10}$); 29.84 (C$_{8, 8`}$); 39.28 (C$_{7,7`}$); 43.41 (C$_{12}$); 51.36 (C$_{11}$); 124.58 (C$_{2,2`}$,C$_{6,6`}$); 126.43 (C$_{3,3`}$, C$_{5,5`}$); 134.34 (C$_{1,1`}$); 137.75 (C$_{4,4`}$); 153.39 (C=N). The electrospray (+) mass spectrum of A_2 showed the mass ion peak at m/z = 347.0251 amu assigned to (M-(CH$_3$)+H)$^+$ for C$_{23}$H$_{29}$N$_3$. Peaks detected at m/z = 303.1755 and 169.1104 were correlated to [(M-(CH$_3$)+(CH$_4$N$_2$)]$^+$ and [(M-(CH$_3$)+(CH$_4$N$_2$)]+(C$_{12}$H$_{14}$)]$^+$.

2.3.2. Synthesis of ligands (H$_2$L^1 and H$_2$L^2)

2.3.2.1. Synthesis of N-(2-(((1R,2R,4R,5S,Z)-2,4-diphenyl-3-azabicyclo[3.3.1]nonan-9-ylidene)amino)ethyl)-2-((2-mercaptoethyl)thio)acetamide (H$_2$L^1)

A mixture of 1,4-dithian-2-one (0.080g, 0.597mmol) in CHCl$_3$ (10ml) was added dropwise, under N$_2$ atmosphere, to a mixture of precursor A$_1$ (0.233g, 0.699mmol) in CHCl$_3$ (10ml). The reaction mixture was stirred under nitrogen atmosphere for 3h. A white solid that formed was collected by filtration, washed with diethylether (10ml) and then allowed to dry under vacuum. Yield: 0.056 g (70 %), m.p. = 312-315 ºC. Ft-IR data (cm^1), 3417 ν(N-H)$_{amide}$, 1662 ν(C=O)$_{amide}$, 1604 ν(C=N), 2555 ν(S-H), 1531 and 1492 ν(C=C)$_{arom}$, 1346 ν(C-N), 1056 and 914 ν(C-S). NMR spectra (ppm), ^{1}H (400 MHz, DMSO-d$_6$), see Figure 1; δ_H = 1.23 (3H, m, H$_{10}$, S-H); 1.60 (2H, t, J_{HH} = 8.8 Hz, H$_{14}$); 1.81 (9H, m, H$_{8,8`}$, H$_{9,9`}$, H$_{11}$ and N-H); 2.61 (2H, t, H$_{15}$, J_{HH} = 6.4 Hz); 2.87(2H, d, H$_{7,7`}$ , $J_{HH}$ = 5.2 Hz); 3.16 (2H, t, H$_{12}$, $J_{HH}$ = 6.4 Hz); 3.63(2H, s, H$_{13}$); 7.44 (2H, t, $J_{HH}$ = 5.2 Hz, H$_{1,1`}$); 7.57 (4H, t, J_{HH} = 5.2 Hz, H $_{2,2`; 6,6`}$); 7.77 (4H, d, J_{HH} = 4.8 Hz, H$_{3,3`; 5,5`}$); 8.09 (1H, s, N-*H*)$_{amide}$.), ^{13}C (100 MHz, DMSO-d$_6$), Figure 2; δc= 24.49 (C$_{10}$); 25.52 (C$_{9,9`}$); 28.80 (C$_{8,8`}$); 32.56 (C$_{15}$); 41.18 (C$_{14}$); 46.42 (C$_{13}$); 48.13 (C$_{12}$); 56.79 (C$_{11}$); 60.97 (C$_{7,7`}$) 125.10(C$_{1,1`}$); 126.95(C$_{2,2`, 6,6`}$);127.11 (C$_{3,3`, 5,5`}$); 138.28 (C$_{4,4`}$); 157.79 (C=N); 175.86 (C=O). The electrospray (+) mass spectrum of H$_2$L^1 showed the parent ion peak at m/z = 467.3040 amu corresponding to (M)$^+$, requires; 467.2065 and the following fragments at 374.2201, 261.1360 and 160.8401 amu were assigned to [M-(C$_2$H$_6$S$_2$)+H]$^+$, [M-(C$_2$H$_6$S$_2$+C$_9$H$_5$)]$^+$ and [M-(C$_2$H$_6$S$_2$+C$_9$H$_5$+C$_5$H$_{11}$NO)]$^+$, respectively.

2.3.2.2. Synthesis of N-(2-(((1R,2R,4R,5S,Z)-2,4-di-p-tolyl-3-azabicyclo[3.3.1]nonan-9-ylidene)amino)ethyl)-2-((2-mercaptoethyl)thio)acetamide(H$_2$L^2)

The method adopted to prepare H$_2$L^2 was similar to that for H$_2$L^1, but with precursor A$_2$ instead of A$_1$. Other reaction reagents were adjusted accordingly and an analogues workup procedure that implemented resulted in the isolation of the required ligand. Yield: 0.2155g (75 %), m.p. = 320-322ºC. IR data (cm^1), 3398 ν(N-H)$_{amide}$, 1674 ν(C=O)$_{amide}$, 1616 ν(C=N), 2619 ν(S-H), 1577and 1523 ν(C=C)$_{arom}$, 1323 ν(C-N), 1033 and 9254 ν(C-S). NMR data (ppm), Figure 1; ^{1}H (400 MHz, DMSO-d$_6$), see Figure 1; δ_H = 1.02 (3H, m, H$_{10}$, S-H);1.582 (2H, t, J_{HH} = 8.8 Hz, H$_{14}$); 1.44 (9H, m, H$_{8,8`}$, H$_{9,9`}$, H$_{11}$ and N-H); 1.71 (2H, t, H$_{15}$, J_{HH} = 6.4 Hz); 2.73(2H, d, H$_{7,7`}$ , $J_{HH}$ = 5.2 Hz); 2.86 (2H, t, H$_{12}$, $J_{HH}$ = 6.4 Hz); 3.09(2H, s, H$_{13}$); 3.59 (2H, t, $J_{HH}$ = 5.2 Hz, 2x CH$_3$); 3.70 (4H, t, $J_{HH}$ = 5.2 Hz, H $_{2,2`; 6,6`}$); 7.15 (4H, d, $J_{HH}$ = 4.8 Hz, H$_{3,3`; 5,5`}$); 7.45 (1H, s, N-*H*)$_{amide}$. ): 8.12. $^{13}$C (100 MHz, DMSO-d$_6$), Figure 2; $\delta$c= 20.40 (C$_{methyl}$); 23.19 (C$_{9,9`}$); 26.35 (C$_{10}$); 28.75 (C$_{8,8`}$); 32.26 (C$_{15}$); 35.46 (C$_{7,7`}$); 41.15 (C$_{14}$); 44.79 (C$_{13}$); 46.14 (C$_{12}$); 54.37 (C$_{11}$); 126.35 (C$_{2,2`, 6,6`}$);128.26 (C$_{3,3`, 5,5`}$); 134.69 (C$_{4,4`}$); 136.69 (C$_{1,1`}$); 146.84 (C=N); 177.69 (C=O). The electrospray (+) mass spectrum of H$_2$L^1 recorded a peak at m/z = 495.2304 amu related to (M)$^+$, requires; 495.2378. Fragments at 403.3873, 374.2201 and 261.1360 amu correspond to [M-(SCH$_2$SCH$_2$)]$^+$, [M-(SCH$_2$SCH$_2$)+(CH$_2$NH)]$^+$ and [M-(SCH$_2$SCH$_2$)+ (CH$_3$NH$_2$)+(NHCCOCHCHCHCH)]$^+$, respectively. Elemental microanalyses of precursors and ligands, colours, yields and melting points are placed in Table 1.
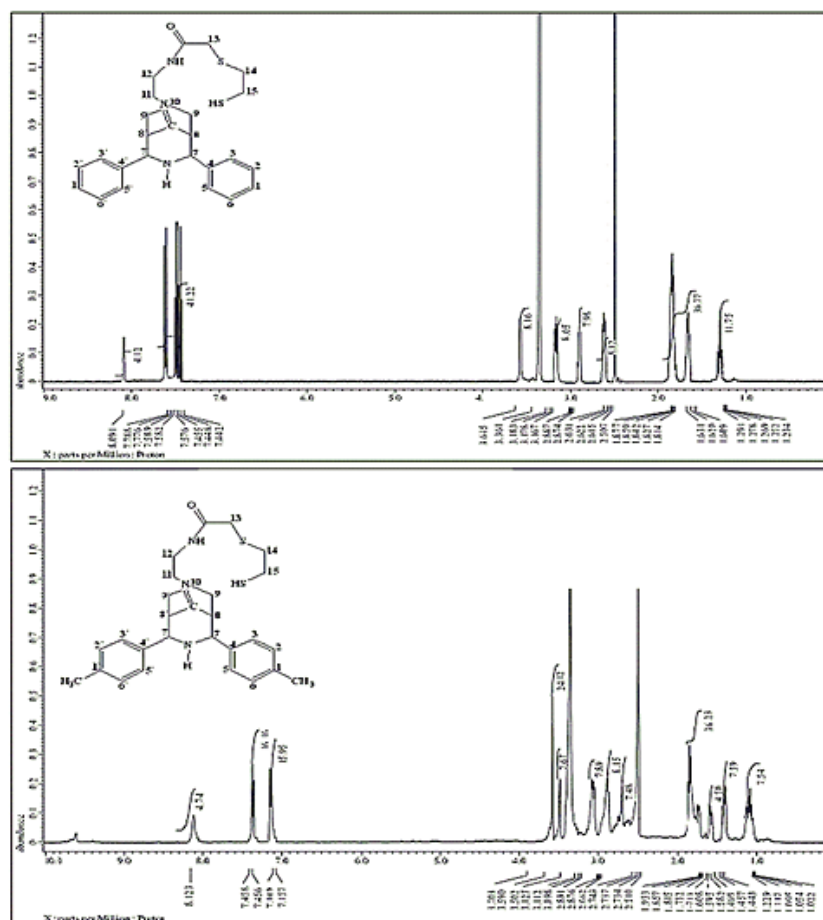
Figure 1. ^{1}HNMR spectra of H_2L^1 and H_2L^2 in DMSO-d_6.
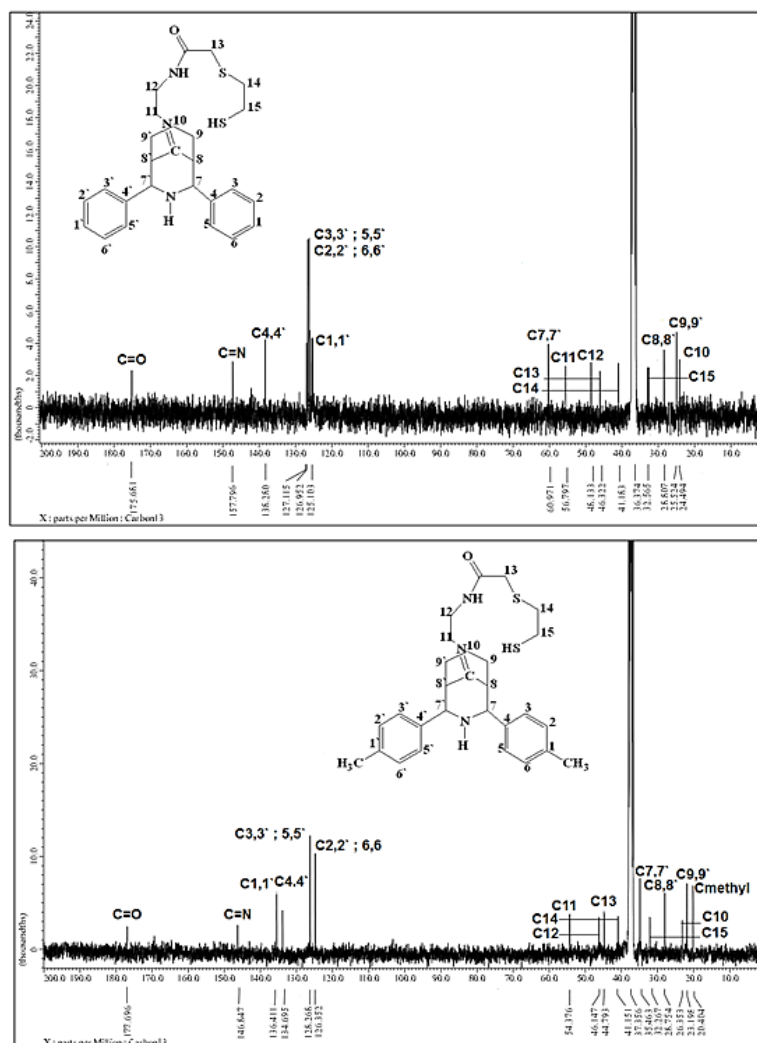
Figure 2. ^{13}CNMR spectra of ligands H_2L^1 and H_2L^2 in DMSO-d_6.

Table 1. Microanalyses data and physical properties for precursors and ligands.

Comp.	Empirical formula	M.wt g/mol	Yield (%)	m.p. °C	Colour	Found/(Calc.)%			
						C	H	N	S
M_1	$C_{20}H_{21}NO$	291.38	93	108-110	White	82.69 (82.44)	7.83 (7.26)	5.03 4.81)	-
M_2	$C_{22}H_{25}NO$	319.44	54	168-170	Pale-yellow	82.24 (82.72)	8.23 (7.89)	4.95 (4.38)	-
A_1	$C_{22}H_{27}N_3$	333.46	65	194-196	Off-white	79.47 (79.24)	8.75 (8.16)	12.98 (12.60)	-
A_2	$C_{24}H_{31}N_3$	361.52	75	113-115	Yellow	80.02 (79.73)	8.17 (8.64)	11.82 (11.62)	-
H_2L^1	$C_{26}H_{33}N_3O S_2$	467.68	70	312-315	White	66.22 (66.77)	7.75 (7.11)	8.44 (8.98)	13.48 (13.71)
H_2L^2	$C_{28}H_{37}N_3O S_2$	495.74	75	320-322	White	67.11 (67.84)	7.95 (7.52)	8.27 (8.48)	12.11 (12.94)

2.3.3. Synthesis of the complexes with H_2L^1 and H_2L^2

A mixture of the title ligand (0.1g, 0.180mmol) in 20ml of a mixture solution of ethanol:chloroform 1:1 and potassium hydroxide (0.03g, 0.541mmol) in ethanol (5ml) was stirred for 10 min. To the above mixture was added dropwise an ethanolic solution (10ml) of the metal chloride (0.043g, 0.180mmol). The resulting mixture was refluxed under N_2 atmosphere for 3h. A solid that formed was filtered, washed by ethanol and diethyl ether, and dried under vacuum. Elemental analysis data, colours, and yields for the ligands and their complexes are given in Table (2).

2.4. Determination of biological activity

The evaluation of compounds (ligands and complexes) against four bacterial strains *(Escherichia coli, Pseudomonas aeruginosa, Staphylococcus aureus and Bacillus)* and four fungi species (*Candida albicans, Candida glabrata, Candida tropicalis* and *Candida parapsilsis*) were performed using agar-well diffusion. In this method, the wells were dug in the media with the help of a sterile metallic borer with centres at least 6 mm. A 100 μL concentration of the title specimen 1 mg/mL in DMSO was placed in the individual wells [13]. The Petri dishes were incubated in the incubator for 24h at 37 ºC. The biological activity was observed by measuring the diameter of inhibition zones (mm).

Table 2. Elemental analyses, some physical properties, yields and colours of (H_2L^1 –H_2L^2) complexes.

Chemical Formula	M.wt g/mol	Yield (%)	Colour	m.p. ºC	μ_{eff} per one atom	Microanalysis Found, (Calc.)%					
						C	H	N	S	M	Cl
$K_2[Mn(L^1)Cl_2]$	699.70	56	Brown	310*	1.85	46.39 (46.58)	4.21 (4.43)	6.68 (6.27)	9.87 (9.55)	8.30 (7.85)	10.02 (10.58)
$K_2[Co(L^1)Cl_2]$	673.70	40	Dark-blue	295*	4.96	46.63 (46.31)	4.36 (4.60)	6.74 (6.23)	9.73 (9.48)	8.11 (8.74)	10.74 (10.52)
$K_2[Ni(L^1)Cl_2]$	673.46	62	Pale-blue	285*	3.83	46.80 (46.32)	4.22 (4.60)	6.64 (6.23)	9.71 (9.50)	8.97 (8.71)	10.67 (10.52)
$[Cu(L^1)]$	529.22	73	Pale-green	250*	1.78	58.39 (58.95)	5.53 (5.85)	8,03 (7.93)	12.71 (12.09)	12.62 (12.00)	00
$[Zn(L^1)]$	531.05	66	White	305*		58.67 (58.75)	5.88 (5.83)	7.92 (7.90)	12.08 (12.05)	12.35 (12.31)	00
$[Cd(L^1)]$	578.09	68	White	315*		54.23 (53.97)	5.82 (5.36)	7.72 (7.26)	11.23 (11.07)	9.86 (9.64)	00
$K_2[Mn(L^2)Cl_2]$	697.76	42	Brown	275*	1.79	48.67 (48.51)	5.27 (5.01)	5.76 (6.01)	9.43 (9.17)	7.48 (7.87)	10.43 (10.16)
$K_2[Co(L^2)Cl_2]$	701.75	71	Green-blue	280*	4.90	47.61 (47.87)	4.51 (4.98)	5.24 (5.98)	9.30 (9.11)	8.82 (8.39)	9.89 (10.10)
$K_2[Ni(L^2)Cl_2]$	701.51	85	Pale-blue	290*	3.31	47.33 (47.89)	4.80 (4.70)	5.22 (5.98)	9.31 (9.12)	8.90 (8.36)	10.23 (10.10)
$[Cu(HL^2)]Cl$	558.28	41	Blue	310*	1.69	60.51 (60.18)	6.65 (6.44)	7.27 (7.52)	11.70 (11.46)	11.72 (11.48)	6.16 6.34

|										
[Zn(L^2)]	559.11	50	White	310*	60.71 (60.09)	6.62 (6.25)	7.72 (7.51)	11.22 (11.44)	11.40 (11.69)	00
[Cd(L^2)]	606.14	68	White	315*	55.17 (55.43)	5.29 (5.77)	6.54 (6.92)	10.29 (10.55)	18.85 (18.54)	00

*= Decomposition temp.

3. Results and discussion

Ligands were prepared from the reaction of amine precursors with 1,4-dithian-2-one. The preparation of the precursors was achieved into two steps; the first step includes Mannich-reaction of benzaldehyde or its derivative with ammonium acetate and cyclohexanone in the presence of ethanol to isolate precursors M_1 and M_2. The second step focused on the reaction of precursors with ethylenediamine to obtain amine compounds A_1 and A_2. The ligands were synthesised from the reaction of 1,4-dithian-2-one and amine precursors in the presence of triethylamine as a base in $CHCl_3$ medium, which gave the title ligands (H_2L^1 and H_2L^2), see Scheme (1). Elemental analysis Table 1, FT-IR (Table 3), NMR (^{1}H- and ^{13}C-NMR) and mass spectra were implemented to determine the entity of compounds (precursors and ligands).

R = H = H$_2$L^1; R = CH$_3$ = H$_2$L^2
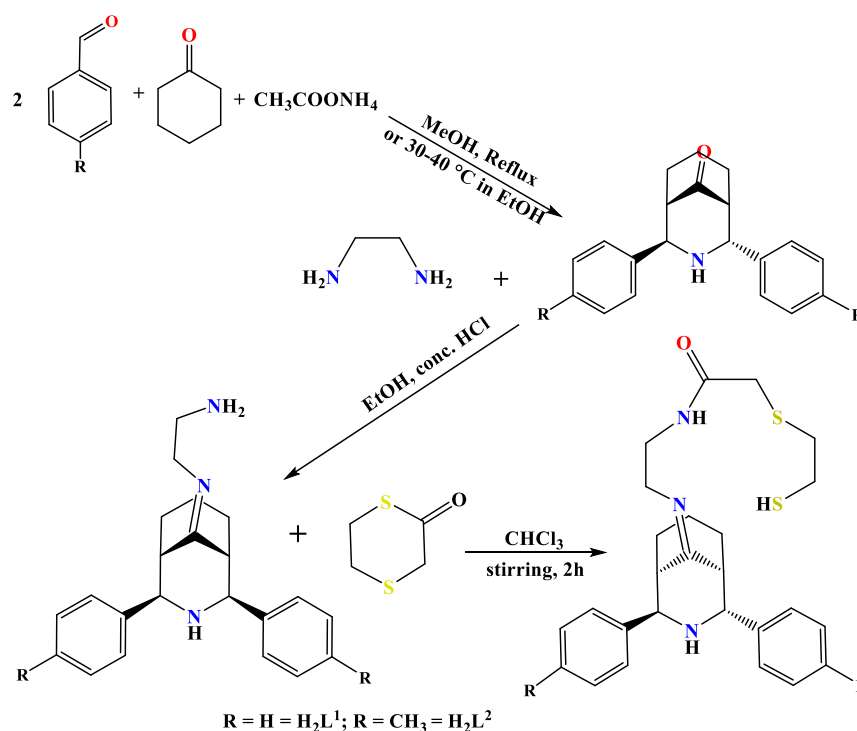
Scheme 1. Synthetic route for precursors and ligands H_2L^1 and H_2L^2.

Complexes of the ligands with Mn(II), Co(II), Ni(II), Cu(II), Zn(II) and Cd(II) ions were synthesised by heating 1 mmole of each ligand with 1 mmole of metal chloride using a mixture of ethanol/chloroform medium at reflux using KOH as a base. In the ethanol/chloroform solution of KOH, the deprotonation of the ligands is occurred that facilitated the formation of $K_2[Co(HL^n)Cl_2]$, $K_2[Mn(HL^n)Cl_2]$, $K_2[Ni(HL^n)Cl_2]$, $[Cu(HL^n)]$, $[Zn(HL^n)]$ and $[Cd(HL^n)]$ (M = Mn(II), Co(II), Ni(II), Cu(II), Zn(II), and Cd(II), $L^n = L^1$ or L^2), Scheme 2. The complexes are air-stable and soluble in DMSO (bar other organic solvents). Elemental analysis and other physical properties of the complexes are placed in Table 4. Physico-chemical data agree well with the proposed formulas. The prominent infrared peaks and their assignments for the ligands and complexes are included in Table 3. The electronic data (UV-Vis) with their assignments for ligands and complexes are placed in Table 4.
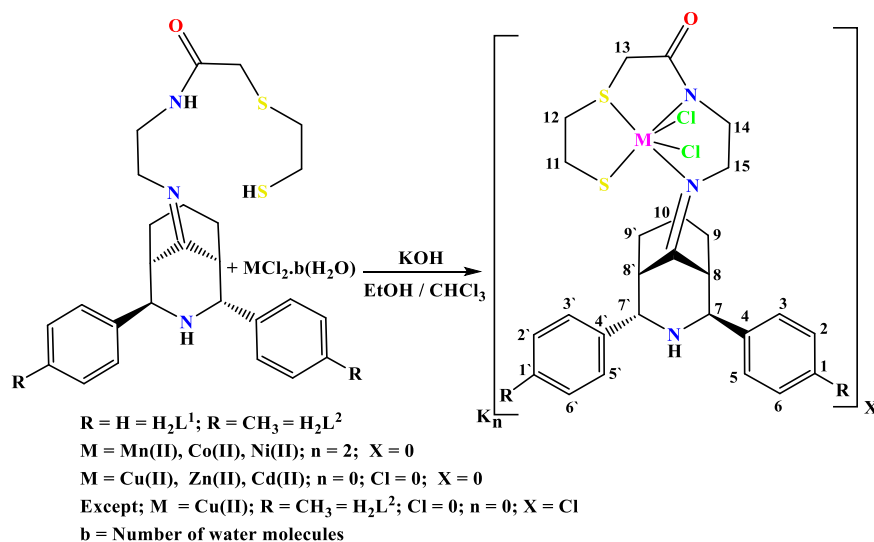
Scheme 2. General synthetic route of (H$_2$L^1 and H$_2$L^2) complexes.

3.1. FT-IR and NMR spectra

The FT-IR spectra of free ligands display bands due to ν(C=O)$_{amide}$, ν(C=N)$_{imine}$ and ν(C-N) groups. The distinct frequency around 2555-2619 cm^1 related to ν(S–H), confirms the presence of the ligands in the thiol form [14]. The FT-IR spectra of the complexes exhibited H$_2$L^1 and H$_2$L^2 bands with the proper shifts due to complex formation (Table 3). Band assigned to ν(S-H) in the free ligands was disappeared in the spectra of complexes, due to the involvement of sulfur atom, as a thiolate moiety, in complex formation. The ν(C=O)$_{amide}$ and ν(C=N)$_{imine}$ at ca. 1662,1674 cm^1 and at ca. 1604-1616 cm^1 in the free ligands were recorded at lower frequencies, indicated a reduced bond order, and observed around 1631-1651; 1600 and 1639-1651; 1600 cm^1 for H$_2$L^1 and H$_2$L^2 complexes, respectively. This shift confirmed the involvement of the N atoms of these moieties in the coordination to the metal centre. Bands detected around 1056-1029; 898-855 cm^{-1} and 1083-1033; 898-855 cm^{-1} were attributed to ν(C-S) for complexes of H$_2$L^1 and H$_2$L^2, respectively indicating the involvement of sulfur atoms upon coordination to metal centre [15]. At lower frequency, the complexes exhibited bands around 416-493 and 333-383 cm^1 attributed to ν(M-N) and ν(M-S), respectively. Bands observed around 244-262 and 243-277 cm^1 in the spectra of K$_2$[Mn(L^1)Cl$_2$], K$_2$[Co(L^1)Cl$_2$], K$_2$[Mn(L^2)Cl$_2$] and K$_2$[Ni(L^2)Cl$_2$] are related to ν(M-Cl) [16]. The appearance of two bands indicated the coordination of the Cl atoms in the *cis* conformation.

Table 3. Infrared spectral data (wavenumber, ν$^-$) cm^{-1} of (H$_2$L^1 - H$_2$L^1) and their complexes

Compound	ν(N-H)	ν(C=O) amid	ν(C=N) imine	ν(C=C) arom	ν(C-N)	ν(C-S)	ν(M-N)	ν(M-S)	ν(M-Cl)
H$_2$L^1	3417	1662	1604	1531 1492	1323	1056 914	-	-	-

$K_2[Mn(L^1)Cl_2]$	3490	1651	1600	1585	1342	1033	470	362	262
				1508		864	428	347	244
$K_2[Co(L^1)Cl_2]$	3485	1631	1600	1581	1338	1029	466	370	254
				1492		891	443	339	248
$K_2[Ni(L^1)Cl_2]$	3500	1651	1600	1504	1342	1033	464		
				1489		860	447		
$[Cu(L^1)]$	3495	1651	1600	1577	1342	1033	493		
				1504		855	455		
$[Zn(L^1)]$	3500	1643	1600	1577	1334	1045	455		
				1500		857	416		
$[Cd(L^1)]$	3500	1647	1600	1585	1330	1064	459		
				1543		898	447		
H_2L^2	3398	1674	1616	1577	1323	1033	-	-	-
				1523		925			
$K_2[Mn(L^2)Cl_2]$	3490	1651	1600	1558	1342	1060	462	383	277
				1508		891	439	333	243
$K_2[Co(L^2)Cl_2]$	3495	1639	1600	1504	1342	1053	479		
				1454		887	439		
$K_2[Ni(L^2)Cl_2]$	3500	1651	1600	1504	1342	1056	462	366	248
				1489		855	439	339	244
$[Cu(HL^2)]Cl$	3302	1647	1600	1570	1342	1083	474		
	3232			1504		879	443		
$[Zn(L^2)]$	3455	1651	1600	1570	1338	1083	466		
				1504		891	443		
$[Cd(L^2)]$	3485	1651	1600	1543	1330	1064	474		
				1504		898	459		

The ^1H and ^{13}C NMR spectra of ligands revealed peaks related to the various proton and carbon nuclei consistent with the proposed structural formula. The ^1HNMR spectrum of $[Cd(L^1)]$ Figure 3; in DMSO-d_6 solution indicated two characteristic sets of chemical shifts in the aliphatic and aromatic regions. In the aromatic region, the spectrum indicated signals at; 7.57 ppm (4H, d, J_{HH} = 4 Hz, $H_{3,3`; 5,5`}$); 7.17 (4H, t, J_{HH} = 8 Hz, $H_{2,2`;6,6`}$); 7.02 ppm (2H, t, J_{HH} = 8 Hz, $H_{1,1`}$). The aliphatic region shows chemical shifts at 3.99 (2H, s, $H_{13}$); 3.41 (2H, t, $H_{12}$, $J_{HH}$ = 8 Hz); 2.68 (2H, s, $H_{7,7}$); 2.34 (2H, t, $H_{15}$); 1.60 (9H, m, $H_{8,8`}$, $H_{9,9`}$, H_{11} and N-*H*); 1.14 (2H, t, H_{14}, J_{HH} = 8 Hz); 1.01 (2H, m, H_{10}). The spectrum indicated no signals may attribute to N-H of the amide groups and S-H of thiol, confirming the involvement of these moieties in complexation, and making the ligand behaves as -2 species upon complexation. 22.61 (C_{10}); 23.50 ($C_{9,9`}$); 28.36 ($C_{8,8`}$) 29.61 (C_{15}); 38.07(C_{14}); 39.81(C_{13}); 41.10(C_{12}) 44.27 (C_{11}); 67.52 ($C_{7,7}$); 128.27($C_{1,1`}$); 128.60 ($C_{2,2`, 6,6`}$); 131.63 ($C_{3,3`, 5,5`}$); 137.43 ($C_{4,4`}$); 167.06 (C=N); 188.12 (C=O). The ^{13}C-NMR spectrum of $[Cd(L^2)]$ displayed signals at; 22.30 (C_{methyl}); 23.80 ($C_{9,9`}$); 28.24 ($C_{10}$); 28.55 ($C_{8,8`}$); 34.49 (C_{15}); 43.95 ($C_{7,7`}$); 50.28 ($C_{14}$); 55.42 ($C_{13}$) and ($C_{12}$); 55.76 ($C_{11}$); 128.21($C_{2,2`, 6,6`}$); ($C_{3,3`, 5,5`}$) 132.55; 134.45 ($C_{4,4`}$); 135.17 ($C_{1,1`}$); 159.76 (C=N); (C=O) 188.87 ppm. The chemical shift for the imine and amide groups by ca. 10-13 and 11-13 ppm, respectively in comparison with that in the free ligand confirmed the involvement of the nitrogen atoms of the imine and amide groups in complexation. This shift is related to the deshielding occurred to these moieties by the Cd(II) centre upon complexation.
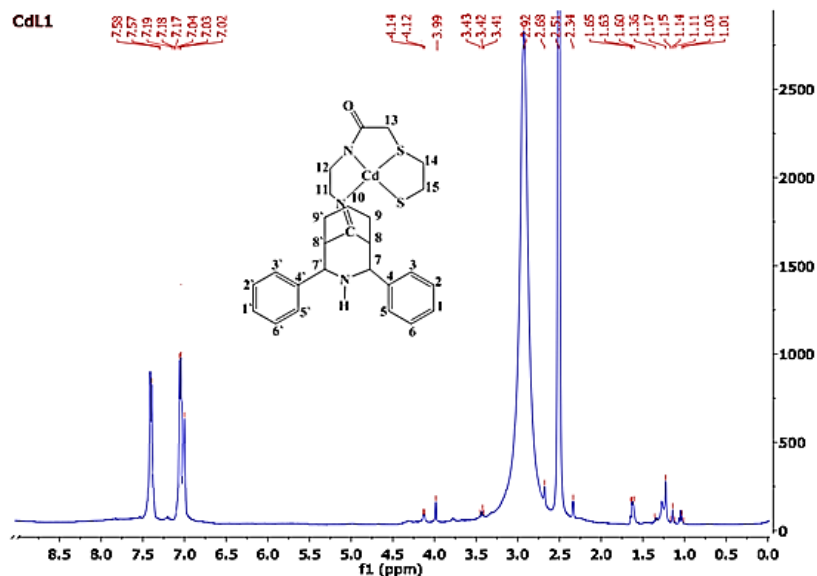
Figure 3. ^{1}HNMR spectrum of [Cd(L^1)] complex in DMSO-d$_6$.

3.2. Mass spectra

The obtained mass spectra of the ligands agreed with the suggested structural formula (see experimental section and 'Figure 4'.
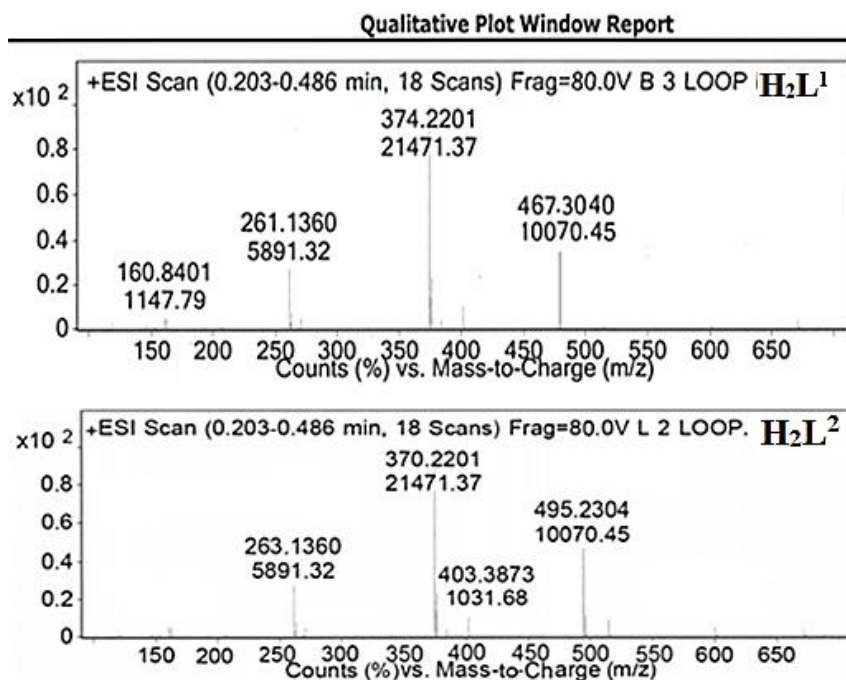

Figure 4 . ESI (+) mass spectra of H$_2$L^1 and H$_2$L^2

The accurate electrospray (+) mass spectrum of K$_2$[Ni(L^1)Cl$_2$] Figure 5; indicated a peak at m/z = 671.4532 amu, requires = 670.9913 corresponding to (M)$^+$. The successive fragments at 487.3041, 374.2202, 261.1360 and 160.8402 were assigned to [M-(C$_5$H$_6$S)+(C$_4$H$_2$S)]$^+$,[M-(C$_5$H$_6$S)+(C$_4$H$_2$S)+(CHCl$_2$NO)]$^+$, [M-(HCN)+(2HCl)+(C$_4$H$_8$S$_2$)+(HCN)+(C$_6$H$_4$O)+(C$_5$H$_2$C$_5$H$_6$S)+(C$_4$H$_2$S)+(CHCl$_2$NO)+(HCN)+(C$_7$H$_2$)]$^+$ and [M-(C$_5$H$_6$S)+(C$_4$H$_2$S)+(CHCl$_2$NO)+(HCN)+(C$_8$H$_3$N)+(C$_6$H$_{13}$N)]$^+$, respectively.
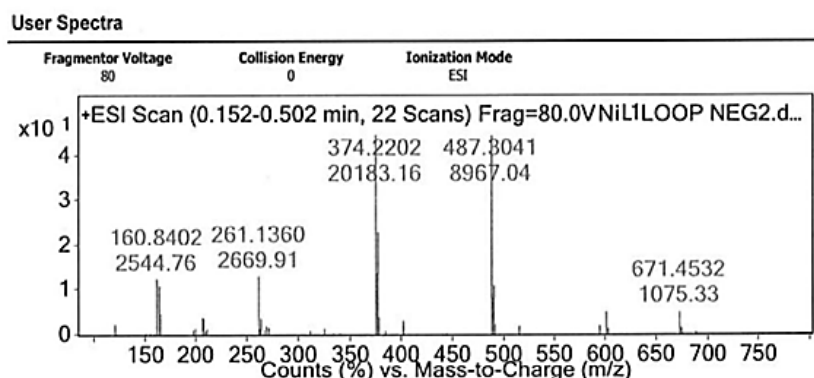
Figure 5. ESI (+) mass spectrum of $K_2[Ni(L^1)Cl_2]$.

3.3. Electronic spectra, magnetic moments, and conductivity measurements

The electronic data of H_2L^1 and H_2L^2 display absorption peak at 260, 265 and 345, 360 nm, respectively related to overlaps of $\pi \rightarrow \pi^*$ and $n \rightarrow \pi^*$ transitions. The spectra of H_2L^1 complexes showed hypsochromic shift peaks correlated to the ligand field transitions ($\pi \rightarrow \pi^*$ and $n \rightarrow \pi^*$) [17-19], bar Cu(II) complex that exhibited a bathochromic shift. The electronic spectrum of Mn(II) complex revealed peaks in the d-d region at 441 and 762 nm assigned to $^6A_1g^{(F)} \rightarrow {}^4T_2g^{(G)}$ and $^6A_1g \rightarrow {}^4T_1g^{(G)}$ transitions, respectively indicating a distorted octahedral geometry about Mn(II) ion [20-21]. These data with the magnetic moment value confirmed an octahedral geometry around the Mn(II) atom. The Co(II) complex displays more peaks in the d-d region at 413, 537 and 674 nm due to $^2Eg \rightarrow {}^2T_1g$ or ^2T_2g, $^2Eg \rightarrow {}^4T_1g^{(F)}$ and $^4T_1g^{(F)} \rightarrow {}^4A_2g^{(F)}$, respectively. This spectrum is characteristic for Co(II) complexes with distorted octahedral geometries around Co atom [22-24]. The μ_{eff} value for this complex is included at the range of octahedral confirming octahedral geometry about metal centre. The Ni(II) complex showed peaks at 417, 610 and 681 nm related to $^3A_2g \rightarrow {}^1T_1g^{(p)}$, $^3A_2g \rightarrow {}^3T_1g^{(p)}$ and $^3A_2g \rightarrow {}^3T_1g^{(F)}$ transitions, respectively confirmed a distorted octahedral geometry around Ni atom [16]. The paramagnetic behaviour of the Ni(II) complex suggested a distorted octahedral geometry. The Cu(II) complex displayed a peak in the d-d region at 828 nm attributed to d-d transition attributed to $^2B_1g \rightarrow {}^2A_2g$, confirming a distorted square planar arrangement about Cu atom [25-27]. The proposed distorted square planar arrangement for the pale-green Cu(II) complex is supported by its magnetic measurement value and other analytical data. The spectra of the Zn(II) and Cd(II) complexes revealed peaks related to ligand field ($\pi \rightarrow \pi^*$ and $n \rightarrow \pi^*$). These diamagnetic complexes (d^{10} system) normally prefer tetrahedral structures. The conductance values of the Mn(II), Co(II), Ni(II), Cu(II), Zn(II) and Cd(II) complexes were in the range of 13.1-76.99 $\Omega^{-1}cm^2mol^{-1}$ indicating 2:1 electrolytic behaviour of the Mn(II), Co(II) and Ni(II), while those of the Cu(II), Zn(II) and Cd(II) complexes were indicating nonelectrolytes [27-28]. The electronic spectra of H_2L^2 complexes revealed peaks that attributed to the ligand field ($\pi \rightarrow \pi^*$ and $n \rightarrow \pi^*$ transitions) [16-18]. The electronic spectrum of Mn(II) complex displayed peaks at 434 and 639 nm correlated to $^6A_1g^{(F)} \rightarrow {}^4T_2g^{(G)}$ and $^6A_1g \rightarrow {}^4T_2g^{(G)}$ transitions, respectively confirming a distorted octahedral structure around Mn atom [23]. These data with the value of magnetic moment support an octahedral geometry around the Mn atom. The Co(II) complex displays additional peaks in the d-d area at 438 and 680 nm due to $^4T_1g^{(F)} \rightarrow {}^4A_2g^{(F)}$ and $^4T_1g \rightarrow {}^4T_2g^{(F)}$ transitions, respectively. This spectrum is characteristic for Co(II) complexes that adopt distorted octahedral structures [23]. The magnetic moment value of the Co(II) complex is in the agreement of octahedral structure with a high spin configuration around Co(II) ion. The Ni(II) complex displayed a peak at 641 nm related to $^3A_2g \rightarrow {}^3T_1g$ transition, confirming a distorted octahedral sphere about Ni atom [23]. The Ni(II) complex is paramagnetic with a value consists of the distorted octahedral geometry. The electronic spectrum of this complex was in agreement with this assignment. Cu(II) complex showed a peak in the d-d region at 794 nm attributed to d-d transition $^2B_1g \rightarrow {}^2B_2g$ demonstrating a distorted square planar geometry about Cu atom [14]. The suggested distorted square planar geometry of the blue Cu(II) complex is supported by magnetic moment value

and other analytical data. The spectra of the Zn(II) and Cd(II) compounds indicated peaks attributed to ligand field ($\pi \rightarrow \pi^*$ and $n \rightarrow \pi^*$). These diamagnetic complexes (d^{10} system) normally prefer tetrahedral structures. The molar conductance values of the Mn(II), Co(II), Ni(II), Cu(II), Zn(II) and Cd(II) complexes were in the range of 7.07-78.21 $\Omega^{-1} cm^2 mol^{-1}$ indicating 2:1 electrolytic behaviour of the Mn(II), Co(II) and Ni(II), while those of the Cu(II), Zn(II) and Cd(II) complexes were indicating nonelectrolytes, except Cu(II) complex that indicated a 1:1 electrolytic behaviour [27-28].

Table 4. Electronic spectral data of (H_2L^1- H_2L^2) complexes in DMSO solutions.

Comp.	Band Position λ_{nm}	Wavenumber (cm^{-1})	Extinction coefficient $\varepsilon_{max(dm^3 mol^{-1} cm^{-1})}$	Assignment	$_M(\Omega^{-1}cm^2mol^{-1})$	Suggested geometry
H_2L^1	285	35087	2197	$\pi \rightarrow \pi$		
	360	27777	545	$n \rightarrow \pi^*$		
$K_2[Mn(L^1)Cl_2]$	275	36363	1146	$\pi \rightarrow \pi^*$	75.08	Distorted
	345	28985	33	$n \rightarrow \pi^*$		Octahedral
	441	22675	32	$^6A_1g \rightarrow {}^4T_2g^{(G)}$		
	762	13123	20	$^6A_1g \rightarrow {}^4T_2g$		
$K_2[Co(L^1)Cl_2]$	269	37174	1724	$\pi \rightarrow \pi^*$	76.99	Distorted
	350	28571	70	$n \rightarrow \pi^*$		Octahedral
	413	24213	72	$^4T_2g^{(F)} \rightarrow {}^4A_2g$ $_{(F)}$		
	537	18621	71			
	674	14836	51	$^4T_2g^{(F)} \rightarrow {}^4A_2g$ $_{(F)}$		
				$^4T_2g^{(F)} \rightarrow {}^4A_2g$ $_{(F)}$		
$K_2[Ni(L^1)Cl_2]$	265	37735	1033	$\pi \rightarrow \pi^*$	74.65	Distorted
	350	28571	36	$n \rightarrow \pi^*$		Octahedral
	417	23980	126	$^3A_2g \rightarrow {}^1T_1g^{(P)}$		
	610	16393	120	$^3A_2g \rightarrow {}^3T_1g^{(F)}$		
	681	14684	206	$^3A_2g \rightarrow {}^3T_1g^{(F)}$		
$[Cu(L^1)]$	290	34482	2312	$\pi \rightarrow \pi^*$	16.77	Distorted
	828	12077	78	$^2B_1g \rightarrow {}^2A_2g$		Square Planar
$[Zn(L^1)]$	264	37878	646	$\pi \rightarrow \pi^*$	14.11	Distorted
	350	28571	48	$n \rightarrow \pi^*$		Tetrahedral
$[Cd(L^1)]$	270	37037	1484	$\pi \rightarrow \pi^*$	13.1	Distorted
	341	29325	53	$n \rightarrow \pi^*$		Tetrahedral
H_2L^2	265	37735	1254	$\pi \rightarrow \pi^*$		
	345	28985	45	$n \rightarrow \pi^*$		
$K_2[Mn(L^2)Cl_2]$	268	37313	1696	$\pi \rightarrow \pi^*$	78.21	Distorted
	350	28571	300	$n \rightarrow \pi^*$		Octahedral
	434	23041	308	$^6A_1g \rightarrow {}^4T_2g^{(G)}$		
	639	15649	25	$^6A_1g \rightarrow {}^4T_2g^{(G)}$		
$K_2[Co(L^2)Cl_2]$	270	37037	1957	$\pi \rightarrow \pi^*$	76.01	Distorted
	438	22831	123	$^4Tg^{(F)} \rightarrow {}^4A_2g^{(F)}$		Octahedral
	680	14705	102	$^4T_1g^{(F)} \rightarrow {}^4A_2g$ $_{(F)}$		
$K_2[Ni(L^2)Cl_2]$	268	37313	1684	$\pi \rightarrow \pi^*$	74.54	Distorted
	350	28571	195	$n \rightarrow \pi^*$		Octahedral
	641	15600	188	$^3A_2g \rightarrow {}^3T_1g^{(F)}$		
$[Cu(HL^2)]Cl$	266	37594	1469	$\pi \rightarrow \pi^*$	32.27	Distorted
	300	33333	45	$n \rightarrow \pi^*$		Square
	794	12594	36	$^2B_1g \rightarrow {}^2B_2g$		Planar
$[Zn(L^2)]$	267	37453	1600	$\pi \rightarrow \pi^*$	13.77	Distorted
	350	28571	75	$n \rightarrow \pi^*$		Tetrahedral
$[Cd(L^2)]$	269	37174	1832	$\pi \rightarrow \pi^*$	7.07	Distorted
	350	28571	85	$n \rightarrow \pi^*$		Tetrahedral

3.4. Thermal gravimetric analysis

This technique was implemented to study the thermal properties of compounds (stability and chemical composition of ligands and some complexes). TGA analysis supported the determination of the melting points of compounds and identifying their decomposition steps, see Table (5). The TGA peak of the ligand Figure 6; observed at 399.9 ℃ indicated the loss of $(C_{20}H_{22}N_2)$ fragment, (det. = 12.364 mg, 60.904 %; calc. = 12.357 mg). The other step occurred at 521.8 ℃ revealed the loss of (CH_3NO) portion, (det. = 1.941 mg, 9.562 %; calc. = 1.921 mg). The third step of the decomposition of the compound at 593.3 ℃ is linked to the evolving of (CH_2S) segment, (obs. = 1.956 mg, 9.633 %; calc. = 1.958 mg). The remaining deposit of the compound above 598.0 ℃ is associated with the loss of (C_4H_6S), (obs. = 4.040 mg, 19.901%; calc. = 3.668 mg). The differences in the weight may be related to a sublimation process that occurred at high temperature. The DSC curve recorded peaks at 317.1, 337.0, 524.1 and 593.3 ℃, which refer to an endothermic decomposition process. While the peak at 344.0 ℃ was referred to an exothermic decomposition process. The exothermic and endothermic peaks may specify combustion of the organic ligand in an argon environment [29-30]. The thermogram for $K_2[Co(L^1)Cl_2]$ Figure 7; which confirmed the Co(II) complex is stable up to 285.0 ℃. In the TGA curve, peak detected at 408.6 ℃ is related to the loss of $(C_7H_4, C_7H_7NO$ and $2HCl)$ segments, (det. = 9.954 mg, 54.997 %; calc. = 9.941 mg). The second step at 594.0 ℃ that indicated the loss of $(2C)$ fragment, (obs. = 0.619 mg, 3.429%; calc. = 0.646 mg). The final residue of the compound that recorded above 598.0 ℃ is correlated to the $(Co, 2K, N_2, 2H_2S, CH_4$ and $C_2H_6)$, (det. = 7.534 41.573 %; calc. = 7.512 mg). The DSC curve indicated peaks at 283.0, 325.4, 353.6, 419.2 and 594.0 ℃ correlated to an endothermic decomposition process. The endothermic peaks may show combustion of the organic ligand in the inert atmosphere [29-30]. The last endothermic peak may indicate the braking of the metal-ligand bond. The thermogram for $[Cu(L^1)]$ Figure 8; which shows the Cu(II) complex is stable up to 220.0 ℃. The TGA peak at 259.9 ℃ attributed to the loss of (C_2H_2) group, (det. = 0.835 mg, 4.347 %; calc. = 0.946 mg). The differences between the observed and calculated weight may be related to the sublimation process. The second step occurred at 391.9 ℃ account for the loss of $(C_4H_6S_2, C_6H_6$ and $NH_3)$ portions, (det. = 7.698 mg, 40.092 %; calc. = 7.711 mg). The third step of the decomposition of the compound is observed at 515.5 ℃, which attributed to the loss of $(2H_2$ and $NH_3)$ fragments, (obs. = 0.771 mg, 4.016 %; calc. = 0.765 mg). The final residue of the compound recorded above 598.0 ℃ is assigned to the $(Cu, HCN$ and $C_{12}H_5NO)$, (obs. = 9.896 mg, 51.543 %; calc. = 9.778 mg). The DSC curve indicated endothermic decomposition processes at temperatures 220.4, 280.4, 334.6 and 515.5 ℃. Peaks at 436.1 and 459.4 ℃ attributed to exothermic decomposition steps. The exothermic and endothermic curves may relate to the combustion of the organic ligand in the inert atmosphere [29-30]. The last endothermic peak may signify the metal-ligand bond breaking. While the thermogram for H_2L^2 is shown in Figure 9; The analysis chart indicated the ligand is intact up to 325.0 ℃. The TGA curve measured at 336.9 ℃ attributed to the mass loss of (C_5H_7NO) segment, (obs. = 3.845 mg, 19.612 %; calc. = 3.844 mg). The second step took place at 399.3 ℃ confirmed the loss of $(C_5H_6S_2, C_5H_5N$ and $C_3H_4)$ portions, (obs. = 12.979 mg, 66.217 %; calc. = 12.985 mg). The third decomposition step of the compound at 577.5 ℃ is assigned to the mass loss of (C_2H_4) fragment, (obs. = 1.146 mg, 5.8471 %; calc. = 1.110 mg). The final residue that observed above 598.0 ℃ is attributed to the elimination of (C_3H_6) portion, (obs. = 1.631 mg, 8.322 %; calc. = 1.664 mg). In the DSC curve, peaks at 331.3, 363.1 and 577.5 ℃ indicate endothermic decomposition processes. Peaks at 535.0 and 568.8 refer to exothermic decomposition processes. The exothermic and endothermic curves may relate to the pyrolysis of the organic ligand in the inert atmosphere [29-30]. The thermogram for $K_2[Mn(L^2)CL_2]$ Figure 10; that revealed the Mn(II) complex is steady up to 272.0 ℃. The TGA curve observed at 399.3 ℃ related to the loss of $(C_5H_6, 2HCl, NH_3, H_2S, C_5H_{10}S$ and $C_7H_8)$ portions, (obs. = 11.014 mg, 55.0305 %; calc. = 11.010 mg). The second and third steps occurred at 485.3 and 580.28 ℃ indicated the evolving of (HCN) compound, (obs. = 0.779 mg, 3.894 %; calc. = 0.779 mg). The final residue of the compound at 598.0 ℃ is related to the loss of $(Mn, 2K, N_2,$ and $C_9O)$, (obs. = 8.215 mg, 41.0755 %; calc. = 8.186 mg). The DSC curve displayed peaks at 272.0, 351.8, 418.3, 449.2, 504.3 and 580.2 ℃ refer to endothermic decomposition processes. The endothermic peaks may relate to the combustion of the organic ligand in an argon environment [29-30]. The last endothermic peak may signify the metal-ligand bond breaking. The thermogram for $K_2[Ni(L^2)Cl_2]$, Figure 11; which revealed the Ni(II) complex is stable up to 288.8 ℃. The TGA peak observed at 411.9 ℃

confirmed the loss of ($C_7H_{11}N$, $C_4H_8S_2$ and C_8H_{10}) segments, (obs. = 10.070 mg, 47.952 %; calc. = 10.069 mg). The second and third step occurred at 443.9 and 594.8 ℃ indicated the loss of (C_2H_4 and HCN) fragments, (det. = 1.663 mg, 7.919 %; calc. = 1.655 mg). The remaining residue above 598.0 ℃ related to the (NiO, 2K, Cl_2, HCN and 4C), (det. = 9.267 mg, 44.128 %; calc. = 8.978 mg). The DSC analysis shows peaks at 288.8, 347.7, 502.7 and 594.8 ℃ refer to endothermic decomposition processes. The peak at 477.0 ℃ refers to an exothermic decomposition step. The exothermic and endothermic peaks may conclude combustion of the organic compound in the inert atmosphere [29-30]. The final endothermic peak attributed to the metal-ligand bond breaking.
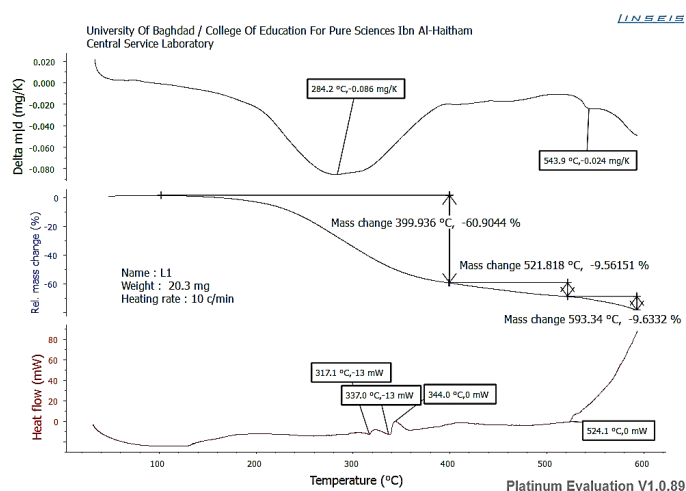

Figure 6. (TGA/ DTA and DSC) thermogram of H_2L^1 in an argon atmosphere.

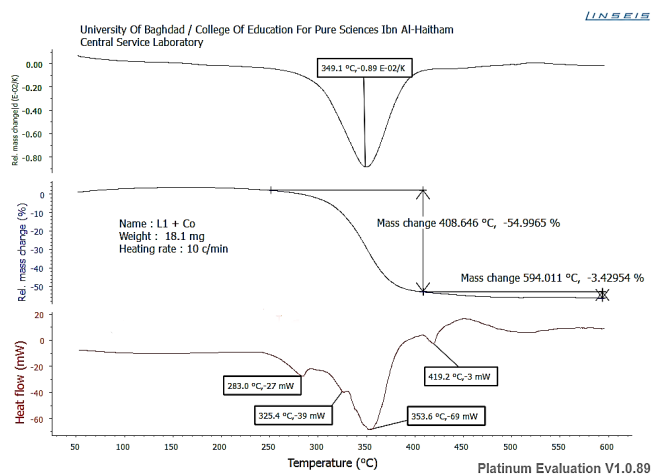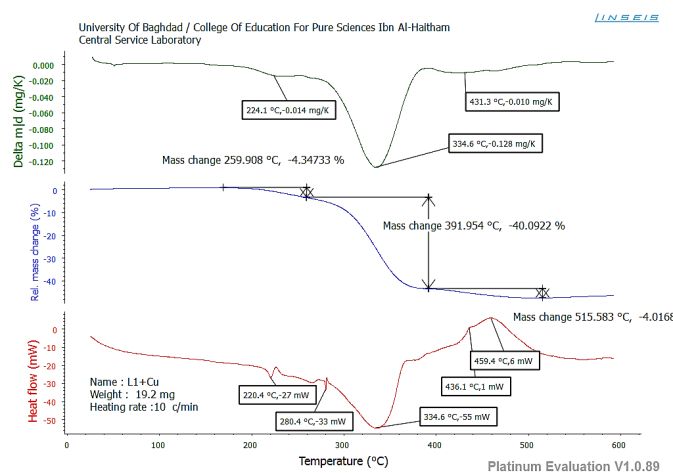**Figure 7 .** (TGA/ DTA and DSC) thermogram of $K_2[Co(L^1)Cl_2]$ in an argon atmosphere**.**

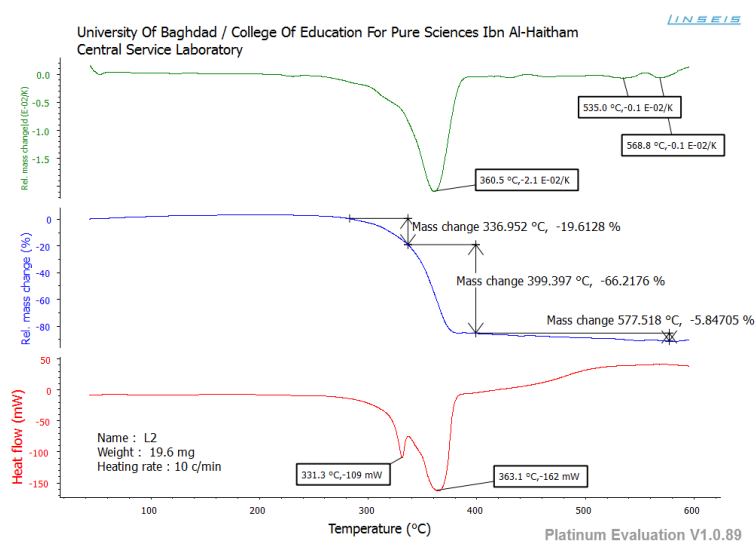**Figure 8.** (TGA/ DTA and DSC) thermogram of [Cu(L^1)] in an argon atmosphere.

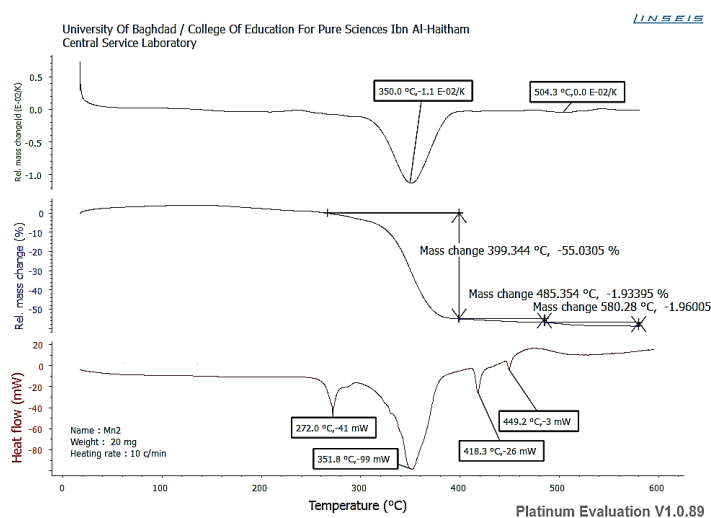**Figure 9.** (TGA/ DTA and DSC) thermogram of ligand H$_2$L^2 in an argon atmosphere.

Figure 10. (TGA/ DTA and DSC) thermogram of K$_2$[Mn(L^2)Cl$_2$] in an argon atmosphere.
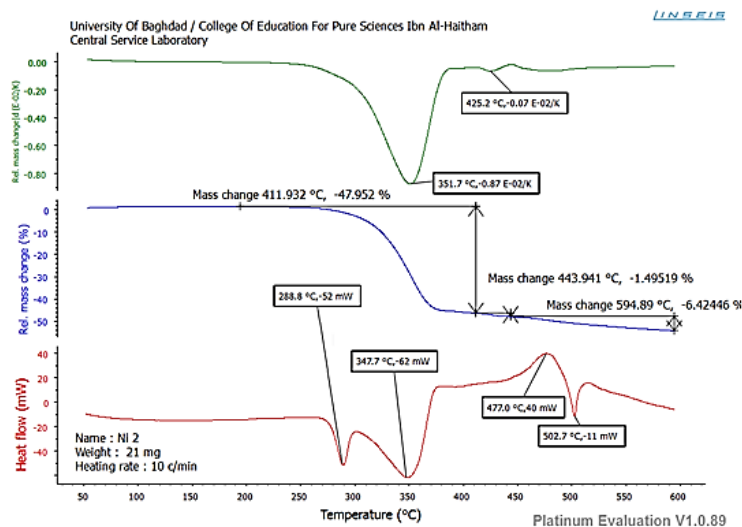
Figure 11. (TGA/ DTA and DSC) thermogram of $K_2[Ni(L^2)Cl_2]$ in an argon atmosphere.

Table 5. TGA/DTA/DSC data for ligands (H_2L^1-H_2L^2) and complexes.

Compound	Stable up to $^\circ$C	Stage	Decomposition temperature $^\circ$C	Nature of transformation/inter mediate formed% mass found (calc.)	Nature of DSC peak and temp. $^\circ$C	DTG peak temp. $^\circ$C
H_2L^1	317.1	1	399.9	12.364 (12.357)	317.1 Endo 337.0 Endo 344.0 Exo	593.3
		2	521.1	1.941 (1.921)		
		3		1.956 (1.958)	524.1 Endo	
$K_2[Co(L^1)Cl_2]$	285.0	1	408.6	9.954 (9.941)	283.0 Enod 325.4 Endo 353.6 Endo 419.2 Endo	594.0
		2	594.0	0.619 (0.646)		
$[Cu(L^1)]$	220.0	1	259.9	0.835 (0.946)	220.4 Endo 280.4 Endo 334.6 Endo 436.1 Exo 459.4 Exo	515.5
		2	391.9	7.698 (7.711)		
		3	515.5	0.771 (0.765)		
H_2L^2	325.0	1	336.9	3.845 (3.844)	331.3 Endo 363.1 Endo Endo	577.7
		2	399.3	12.979 (12.985)		
		3	577.7	1.146 (1.110)		
$K_2[Mn(L^2)Cl_2]$	272.0	1	393.3	11.014 (11.010)	272.0 Endo 351.8 Endo 418.3 Endo 449.2 Endo 504.3 Exo	580.2
		2+3	485.3 and 580.2	0.779 (0.779)		
$K_2[Co(L^2)Cl_2]$	284.8	1	406.2	9.774 (9.784)	284.8 Endo 325.8 Endo 419.0 Endo 513.8 Endo	595.7
		2	595.7	0.619 (0.621)		
$K_2[Ni(L^2)Cl_2]$	288.8	1	411.9	10.070 (10.069)	288.8 Endo 347.7 Endo 477.0	594.3
		2+3	443.9 and 594.3	1.663 (1.655)		

17

Exo
502.7
Endo

4. Antimicrobial activity

The compounds (ligands and complexes) were screened against four bacterial strains (*Escherichia coli, Pseudomonas aeruginosa, Staphylococcus aureus and Bacillus*) and four fungi species (*Candida albicans, Candida glabrata, Candida tropicalis* and *Candida parapsilsis*). The measured areas of inhibition against the growth of different microorganisms were listed in Tables (6 and 7). These data show the inhibition capacity of the prepared compounds on the tested bacteria and fungi species. It is found that metal complexes have antimicrobial activity against bacterial strains and fungi species. This attributed to the complexation influence that allows the participation of the inherent positive charge of the metal ion in complexes with the negative charge provided by the donor atoms of the ligand. Subsequently, the π-electron will distribute over the entire chelate ring resulting in the increases of the lipophilic character of the metal chelate system. This shall help its mobility through the cell membranes [31-32].

Table 6. The bacterial activity of (H_2L^1 - H_2L^2) and their complexes.

| No. | Compound | Gram-negative (G−) | | | | Gram-positive (G+) | | | |
| | | Escherichia coli | | Pseudomonas aeruginosa | | Bacillus stubtilis | | Staphylococcus aureus | |
		Av.	SD±	Av.	SD±	Av.	SD±	Av.	SD±
1	Control	---		---		---		---	
2	H_2L^1	---	0	11.67	1.65	10	7.07	10	0
3	$K_2[Mn(L^1)Cl_2]$	5	1.18	9.33	0.24	12	2.83	17.33	1.18
4	$K_2[Co(L^1)Cl_2]$	14.5	0	14.33	0.47	0	0	0	0
5	$K_2[Ni(L^1)Cl_2]$	19.67	0.24	12.00	0.71	4	5.66	10.33	0.24
6	$[Cu(L^1)]$	13.67	2.36	11.33	0.94	9.67	3.77	13.67	2.36
7	$[Zn(L^1)]$	14	1.41	0	0	14.33	0.47	11.33	1.15
8	$[Cd(L^1)]$	44.67	2.01	21.33	1.08	25	0	36.67	0.76
9	H_2L^2	0	1.65	16.67	1.02	16.67	0	17	0.71
10	$K_2[Mn(L^2)Cl_2]$	6.67	9.43	6.67	0.24	6.67	2.36	16.67	0.24
11	$K_2[Co(L^2)Cl_2]$	3.67	2.60	3.67	0	4.33	3.06	0	0
12	$K_2[Ni(L^2)Cl_2]$	15.67	2.60	15.67	0.24	3	4.24	9.33	0.47
13	$[Cu(HL^2)]Cl$	14.67	6.60	14.67	4.01	0	0	9	1.41
14	$[Zn(L^2)]$	15	0	15	0	10	2.83	14	1.41
15	$[Cd(L^2)]$	23.67	0.94	23.67	1.18	12	0.71	15.67	3.77

5. Conclusions

In the present publication, we have investigated the synthesis, structural characterisation and coordination bonding mode of metal complexes isolated from the reaction of multidentate N_2S_2 heterocyclic ligands (H_2L^1 and H_2L^2) with a range of metal ions. The coordination chemistry and overall structure of the complexes were concluded using a range of analytical and spectroscopic techniques. Further, thermal properties of the ligands and some complexes were established using TGA, DTA and DSC analyses. Biological activities revealed that the ligands and their metal complexes showed different

activity effect on both types of the Gram-positive (G+) and Gram-negative (G-) of the tested bacteria and four species of fungi.

Table 7. Fungi activity of ligands and their complexes.

No.	Compound	*Candida albicans*	*Candida glabrata*	*Candida tropicalis*	*Candida parapsilsis*
1	Control	0	0	0	0
2	H_2L^1	0	13	10	13
3	$K_2[Mn(L^1)Cl_2]$	0	14	10	10
4	$K_2[Co(L^1)Cl_2]$	0	10	18	20
5	$K_2[Ni(L^1)Cl_2]$	8	22	19	16
6	$[Cu(L^1)]$	0	14	11	15
7	$[Zn(L^1)]$	0	10	18	0
8	$[Cd(L^1)]$	8	24	33	30
9	H_2L^2	0	0	0	0
10	$K_2[Mn(L^2)Cl_2]$	0	13	15	16
11	$K_2[Co(L^2)Cl_2]$	0	0	18	12
12	$K_2[Ni(L^2)Cl_2]$	9	11	0	10
13	$[Cu(HL^2)]Cl$	0	0	16	12
14	$[Zn(L^2)]$	0	12	10	15
15	$[Cd(L^2)]$	13	22	22	22

References
[1] Asatkar A K, Tripathi M, Panda S, Pande R and Zade S S 2017 *Spectro Chimica Acta Part A: Molecular and Biomolecular Spectroscopy,* **171**, 18.
[2] Thaddeus J W , Edward H W, Gary R W and Carolyn J 2010 *A. Chem. Rev.,* **110**, 3, 2858.
[3] Abram U and Alberto R 2006 *J. Braz. Chem. Soc.,* **17**, 8, 1486.
[4] Yokoi A , Yoshinari N and Konno T 2015 *J. Incl. Phenom. Macrocycl Chem.*, **82**, 123.
[5] Bilgin A, Ertem B, Gok Y 2009 *Dyes and Pigments,* **80**, 1, 187.
[6] Al-Rubaye B K, Brink A, Miller G J, Potgieterd H Al-Jeboori M J 2017 *Acta Cryst*. **E73**, 1092.
[7] Al-Rubaye B K, Potgieter H and Al-Jeboori M 2017 *J Der Chemica Sinica*, **8** (3)**,** 365.
[8] Al-Jeboori M J 1996 , Novel Rhenium, *Technetium and Nickel Complexes as Radiopharmaceuticals in Nuclear Medicine,* Technical University of Munich. *Germany,* PhD.
[9] Archer C M, Dilworth J R, Griffiths D V, Al-Jeboori M J, Kelly J D, Lu C, Rossera M J and Zheng Y 1997 *J. Chem. Soc., Dalton Trans.,*1403.
[10] Al-Jeboori M J , Al-Fahdawi M S and Sameh A A 2009 *J. Coord. Chem.,* **62**, 3853.
[11] Umamatheswari S and Kabilan S 2011 *J. Enzyme Inhib. Med. Chem.* **26**, 430.
[12] Sampath N, Malathy S S M, Ponnuswamy M N and Nethaji M 2004 *Cryst. Res. Technol.,* **39**, 821.
[13] Rahman A, Choudhary M and Thomsen W 2001 *Bioassay Techniques For Drug Developmen*", Harwood Academic. Amsterdam. The Netherlands.
[14] Al-Jeboori M J, Al-Tawel H H and Ahmad R M 2010 *Inorganica Chimica Acta,* **363**, 1301.
[15] Ferreiraa G B, Comerlatoa N M , Wardell J L and Hollauer E 2004 *J. Braz. Chem. Soc.,* **15**, 951.
[16] Abdul-Gganiy A J , AL-Jeboori M J and Al-karawi J A 2009 *Journal of Coordination Chemistry*, **62**, 2736.
[17] Orescanin V , Mikelic L , Roje V and Lulic S 2006 *Anal. Chim. Acta.,***570**, 277.
[18] Jowit T R N and Mitchell P C H 1970 *J. Chem. Soc.* part A, 1702.

[19] Ronconi L , Giovagnini L, Marzono C, Bettio F , Graziani R , Pilloni G and Fregona D 2005 *Inorg. Chem,* **44** 1867.

[20] El-Sonbati A Z , Al-Shihri A S and El-Bindary A A 2004 *Spectro chimica Acta Part A: Molecular and Biomolecular Spectroscopy*, **60**(8-9) 1763.

[21] Al-Jeboori F H A, Hammud K K , Al-Jeboori M J 2014 *Iranian Journal for Science & Technology*, **38A** (4) 489.

[22] Yousif N S , Hegab K H and Eid A E 2003 , *Inorganic and nano- metal chemistry,* **33** 1647.

[23] Ahmad R M 2012 *Synthesis, Characterisation and Theoretical Studies of Polymeric Chain-Assemblies of Transition Metal Complexes with Mixed Azido-Carboxylato Bridges*, University of Baghdad, College of Education - Ibn-Al-Haitham, PhD .

[24] Lever A B P 1984 *Inorganic Electronic Spectroscopy* 2nd ed., New York.

[25] Baghlaf A O , Ishaq M , Ahmed O A and Al-Julani M A 1985 *Polyhedron*, **4** 853.

[26] Jowitt R N and Mitchell P C H 1970 *J. Chem. Soc.* part A, 1702.

[27] Canpolat E and Kaya M 2005 *J. Coord. Chem.,* **31** 511.

[28] Geary W J 1971 *Russian J. Coord. Chem. Rev.,***7** 81.

[29] Yousif E I, Hasan H A , Ahmad R M , Al-Jeboori M J 2016 *Der Chemica Sinica*, 7(2) 53.

[30] Muat T H , Al-Jeboori M J 2016 *Chem Xpress*, **9** 156.

[31] Singh R V , Dwivedi R and Joshi S C 2004 , *Trans .Met .Chemi,* **29** 70.

[32] Tweedy B G 1964 *Phytopathology,* **55** 910.